Journal of Quantitative Spectroscopy & Radiative Transfer 111 (2010) 1921–1930

Contents lists available at ScienceDirect

Journal of Quantitative Spectroscopy & Radiative Transfer

journal homepage: www.elsevier.com/locate/jqsrt

Optical properties of mixed phase boundary layer clouds observed from a tethered balloon platform in the Arctic

M. Sikand [a,*], J. Koskulics [a], K. Stamnes [a], B. Hamre [b], J.J. Stamnes [b], R.P. Lawson [c]

[a] Department of Physics, Stevens Institute of Technology, 1 Castle point, Hoboken, NJ 07030, USA
[b] Department of Physics and Technology, University of Bergen, Allégaten 55, Bergen, Norway
[c] SPEC Incorporated, 3022 Sterling Circle, Suite 200, Boulder, CO 80301, USA

ARTICLE INFO

Article history:
Received 9 January 2010
Received in revised form
6 March 2010
Accepted 8 March 2010

Keywords:
Mixed-phase clouds
Radiative transfer
DISORT
Snow

ABSTRACT

A tethered balloon system was used to collect data on radiometric and cloud microphysical properties for mixed phase boundary layer clouds, consisting of ice crystals and liquid water droplets during a May–June 2008 experimental campaign in Ny-Ålesund, Norway, located high in the Arctic at 78.9°N, 11.9°E. The balloon instrumentation was controlled and powered from the ground making it possible to fly for long durations and to profile clouds vertically in a systematic manner. We use a radiative transfer model to analyze the radiometric measurements and estimate the optical properties of mixed-phase clouds. The results demonstrate the ability of instruments deployed on a tethered balloon to provide information about optical properties of mixed-phase clouds in the Arctic. Our radiative transfer simulations show that cloud layering has little impact on the total downward irradiance measured at the ground as long as the total optical depth remains unchanged. In contrast, the mean intensity measured by an instrument deployed on a balloon depends on the vertical cloud structure and is thus sensitive to the altitude of the balloon. We use the total downward irradiance measured by a ground-based radiometer to estimate the total optical depth and the mean intensity measured at the balloon to estimate the vertical structure of the cloud optical depth.

1. Introduction

Long-lived thin stratus clouds play an important role in the radiation budget of the polar regions. Thus, it is important to validate radiometric measurements and microphysical properties of clouds obtained remotely via satellite instruments and *in situ* by instruments deployed on aircrafts. Whereas aircrafts are limited by flight durations and satellite observations are hampered by low contrast between cloud and snow/ice covered surfaces in the visible and temperature inversions in the infrared spectral range, a tethered balloon system (TBS) can collect *in situ* data on radiometric and microphysical properties of clouds for days at a time. In this pilot project, mixed phase boundary layer clouds, consisting of ice crystals and liquid water droplets, were observed with instruments deployed on a tethered balloon platform during a May–June 2008 experimental campaign in Ny-Ålesund, Norway, located high in the Arctic at 78.9°N, 11.9°E. The balloon instrumentation was controlled and powered from the ground providing a unique ability to fly for long durations and to profile clouds vertically in a systematic manner.

The solar radiation field in a cloudy earth atmosphere is strongly influenced by scattering and absorption by cloud particles as well as by the albedo of the underlying surface [1]. The optical properties of clouds needed in radiative transfer simulations are the optical depth, the single-scattering albedo and the scattering phase function of

* Corresponding author. Tel.: +1 201 290 3882.
E-mail addresses: Monika.Sikand@stevens.edu, monikavsikand@gmail.com (M. Sikand).

0022-4073/$ - see front matter © 2010 Elsevier Ltd. All rights reserved.
doi:10.1016/j.jqsrt.2010.03.002

cloud particles. Clouds may consist of liquid water droplets or ice crystals, or a mixture of liquid water and ice particles (mixed phase). Clouds exhibit large variations in phase and optical properties on both small and large scales and are challenging to treat realistically in radiative transfer models (RTMs), particularly in RTMs employed in climate modeling. Reliable knowledge of cloud microphysical and radiative properties, which is crucial for the radiative transfer and energy budgets [2], is required to improve the accuracy of climate predictions and enhance key observation networks in the polar regions.

While the relative radiative influence of water droplets and ice particles can be simulated numerically, there has been a relative dearth of reliable *in situ* measurements of vertical profiles of water and ice portions of mixed-phase clouds in the Arctic. The 1998 NSF Surface Heat and Energy Budget of the Arctic (SHEBA) project, combined with NASA's First ISCCP Regional Experiment (FIRE) Arctic Cloud Experiment (ACE) project provided the first aircraft measurements from which water and ice crystal particle size distributions could be reliably separated using cloud particle imager (CPI) data [3]. After SHEBA/FIRE.ACE the only field campaign with CPI data focusing on aircraft measurements of arctic clouds is the Mixed-Phase Arctic Cloud Experiment (M-PACE) conducted on the North Slope of Alaska in September/October of 2004 by the Department of Energy (DOE) Atmospheric Radiation Measurement (ARM) Program [4].

Based upon the lessons learned from SHEBA/FIRE.ACE and M-PACE, a TBS was developed and deployed to study mixed-phase clouds in Ny-Ålesund Svalbard, Norway (78.9°N, 11.9°E) in May/June 2008 with support from the Atmospheric Division of NSF and the Norwegian Research Council through its International Polar Year programme and the project IPY-THORPEX. The TBS instrument package included basic meteorological sensors as well as miniaturized microphysical and radiation sensors [5]. The data collected by the meteorological sensors included pressure, temperature, humidity, wind speed and wind direction. Radiation measurements were made using a 4π radiometer that simultaneously measured irradiances at 500 and 800 nm on the six sides of a cube, measurements that can be used to estimate the mean intensity. Microphysical data were obtained using a miniaturized version of an airborne cloud particle imager (CPI). The TBS can be used to make vertical profiles of a cloud from the balloon's maximum height all the way down to the surface and unlike aircraft, to cover the full vertical extent of most boundary-layer arctic clouds. Depending on horizontal wind speed relative to the vertical profiling speed of the balloon, the profile provided by the TBS relative to a moving cloud is nearly vertical, unlike aircraft profiles, which are either slant or spiral, thus mixing regions of clouds over horizontal scales of several kilometers. The Ny-Ålesund deployment demonstrated the utility of the TBS as an observing system capable of making long-term, cost-effective measurements of the microphysical and radiative properties of clouds in the Arctic.

Climate change appears to be more pronounced in the Arctic than in other regions of the globe [6] and it has gradually become clear that the Arctic is much more important for the global climate than had been appreciated. Therefore, an interagency Study of Environmental Arctic Change (SEARCH) program was developed to observe changes in the arctic climate. Although future projections from global climate models vary, there is broad agreement that the arctic ice cover will shrink considerably. The Barents Sea and the area around Svalbard are crucial due to feedback mechanisms and high variability in the sea ice cover. The data collected by the TBS can be used to investigate how the optical properties of mixed-phase clouds will influence the radiation budget and thereby climate change in the Arctic.

In this paper, we attempt to understand the optical properties of mixed-phase clouds by analyzing the radiometric measurements from the Ny-Ålesund campaign with the help of a state-of-the-art radiation transfer model based on DISORT [7]. The radiometric TBS measurements obtained for a clear-sky situation on May 4, 2008 and cloudy situation on May 29, 2008 were analyzed for this purpose. These measurements consist of mean intensity data collected at 500 and 800 nm with a 4π radiometer deployed as part of the TBS and downward irradiances measured at the ground with a spectrometer. The mean intensity and the total downward irradiance measurements obtained under cloudy conditions on May 29, 2008 were compared with model simulations for the coupled atmosphere-surface (snow/ice, open water) system. The subsequent analysis helped us estimate the mixed phase cloud optical properties, such as optical depth, single-scattering albedo and asymmetry factor. The maximum cloud optical depth estimated from a good match between measured and simulated radiometric data was found to be approximately 31 at 500 nm and approximately 32 at 800 nm. We also found the total downward irradiance at the ground not to be very sensitive to the vertical distribution of the cloud optical depth as long as the total optical depth remained unchanged. The mean intensity and downward irradiance were found to be most sensitive to the single-scattering albedo of the cloud particles.

In Section 2, the instrumentation deployed on the balloon and at the ground is described. Section 3 describes the radiometric measurements. In Section 4, we discuss the radiative transfer model and its inputs in terms of cloud optical properties, which were chosen to be consistent with the CPI cloud particle data. Section 5 discusses the results. Finally, in Section 6, we provide a summary along with an outlook on the future use of the TBS in atmospheric studies of optical properties of mixed-phase clouds.

2. Instrumentation

The TBS instruments used in this study were deployed on a balloon (see Fig. 1) to measure meteorological parameters, cloud particle microphysical characteristics and radiometric parameters. The radiometric measurements to be focused on in this paper were made with a lightweight two-channel moderate bandwidth filter instrument, named NILU-CUBE,

as the TBS was flown to an altitude of about 1400 m on a clear-sky day and 1200 m on a cloudy day. The 4π radiometer, designed and constructed by the Norwegian Institute of Air Research (NILU), was refurbished and carefully tested before launch [8]. Fig. 2 provides a close-up view of the NILU-CUBE instrument, which consists of six sensors mounted on the faces of a cube, each sensor measuring the irradiance in two channels, centered at approximately 500 and 800 nm and having a full width at half maximum (FWHM) of approximately 10 nm, as shown in Fig. 3. Data were recorded every two seconds and stored in a separate logging unit.

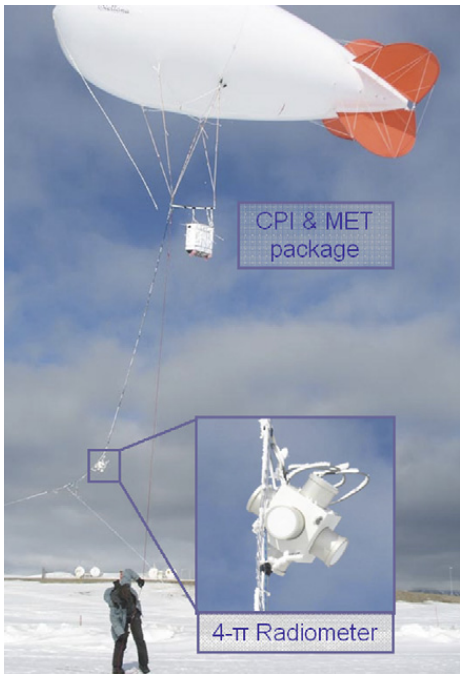

Fig. 1. The TBS with instrumentation attached to the tether of the balloon. The container directly beneath the balloon houses the meteorological (MET) package and cloud particle imager (CPI). The 4π radiometer is attached to the tether 10 m beneath the balloon.

During flight the NILU-CUBE should ideally be mounted such that one sensor would face approximately upwards measuring downwelling radiation, while the opposite sensor would measure upwelling radiation. Then the remaining four sensors would point approximately towards the horizon. In reality the NILU-CUBE was attached to the tether in one corner as shown in Fig. 1. As the balloon ascended, the payload would rotate, so that the signal measured by the six sensors would vary considerably. The radiance incident from all directions contributes to the actinic flux, defined as the incident radiation integrated over all solid angles, which is the same as 4π times the mean intensity. The details of the calibration and orientation effects of the measurements are discussed in Koskulics et al. [8].

3. Measurement results

3.1. Clear sky balloon measurements obtained on May 4, 2008

The meteorological package below the balloon (see Fig. 1) collected ancillary meteorological data (pressure, temperature, humidity, wind speed and wind direction) to support the cloud particle measurements as well as to provide real-time information to aid in positioning the TBS at altitudes of interest. A cloud particle imager (CPI) [9] was used to collect high resolution images of water drops and ice particles in clouds. The CPI (Fig. 4) records images of cloud particles, which can be used to determine particle sizes and shapes and to determine the asymmetry factor for each cloud layer. Before launch of the TBS each irradiance measuring sensor was calibrated outdoors by comparison with irradiance data measured by a co-located reference instrument (TriOS RAMSES-ACC-UV Hyperspectral UV/VIS Irradiance sensor), which was pointing towards zenith to measure the total downward irradiance (for details see Koskulics et al. [8]).

On the clear-sky day of May 4, 2008 (Fig. 5) the flight started at 16:49:50 UTC and lasted till 20:23:38 UTC. The NILU-CUBE instrument in the balloon recorded data every 2 s and Fig. 5 shows the vertical profile of the clear-sky mean

Fig. 2. NILU-CUBE moderate bandwidth filter instrument consisting of six sensors mounted on the faces of a cube.

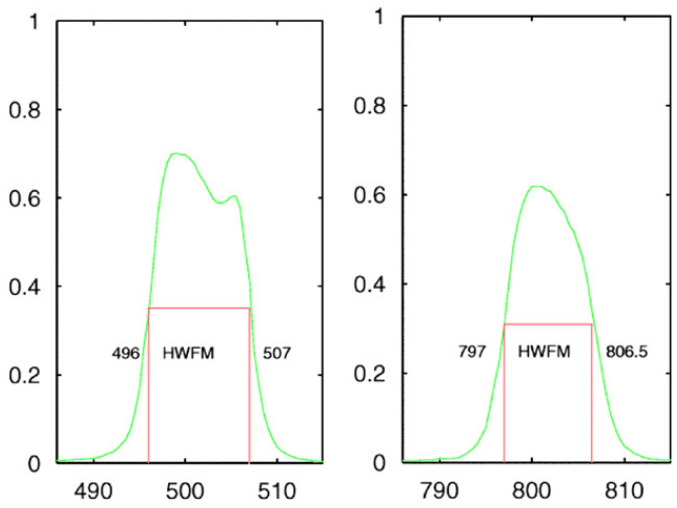

Fig. 3. NILU-CUBE detector filter response for the 500 nm (left) and the 800 nm channel (right).

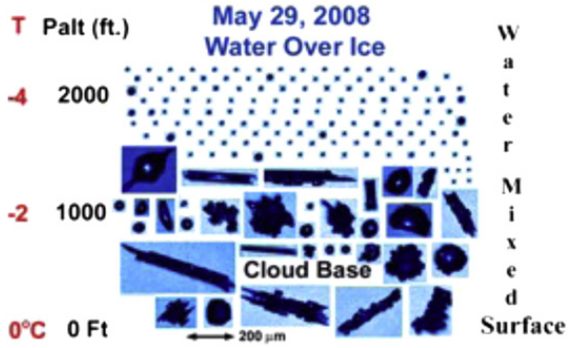

Fig. 4. Cloud particle imager (CPI) data obtained on May 29, 2008.

intensity measured under clear sky conditions at different solar zenith angles during the flight. As mentioned previously, the NILU Cube instrument measured the hemispherical irradiance in six mutually orthogonal directions normal to the surfaces on a cube. These hemispherical irradiances depend on the orientation of the instrument relative to a potential dominant direction of the radiation field, which would give the instrument directional sensitivity when measuring an anisotropic radiation field. The small kinks, such as the one seen around an altitude of 800 m in Fig. 5, are attributed to the directional sensitivity of the NILU-CUBE instrument. The reduction in mean intensity with altitude is due to the effective surface albedo being larger when the instrument is close to the snow covered surface. As the balloon ascends, darker areas including open water and buildings tend to reduce the effective ground albedo and thus decrease the mean intensity. Some outliers in the plot could be attributed to computer generated errors in the collection of the data from the instrument.

3.2. Cloudy sky balloon measurements obtained on May 29, 2008

On the cloudy day of May 29, 2008 the flight started at 10:45:02 and lasted till 15:25:06 UTC. As shown in Fig. 6, the balloon flew up to approximately 1200 m and different values of the mean intensity were found below and above the cloud. Madronich [10] and de Arellano et al. [11] predicted that lower mean intensity values would be found inside a cloud than in clear-sky conditions and that the mean intensity would increase with altitude in a cloud to reach a maximum value near the cloud top. Fig. 6 shows that on May 29, 2008 there was a general increase in the mean intensity with altitude and that this increase was fairly large between 400 and 700 m and even larger between 700 and to 1200 m, where maximum mean intensity values of nearly 300 and 167 $mW\,m^{-2}\,nm^{-1}$ were recorded in the 500 and 800 nm channels, respectively. The behavior seen in Fig. 6 of the mean intensity in the presence of clouds is consistent with an enhancement of the diffuse radiation due to multiple scattering [10]. This enhancement varies with altitude because of variations during the time of flight of the solar zenith angle and also of cloud characteristics, such as cloud-base and cloud-top height, as well as cloud optical depth. During the descent, Fig. 6 shows a significant reduction in the mean intensity between 1200 and 800 m and a smaller reduction between 700 and 400 m. These changes could again be due to the changing cloud conditions during the time of flight. Again, some outliers in the plot could be due to computer generated errors in the collection of data from the instrument. The difference between the two wavelength channels in terms of radiative transfer lies mainly in the scattering and absorption properties of the cloud-free molecular atmosphere. Thus, there is slightly more absorption in the 800 nm channel. In the future we would like to explore the benefit of adding channels in the near infrared beyond 800 nm. The scattering and absorption properties of snow are also different at the two wavelengths. Finally, the solar irradiance at the top of the atmosphere has different values at these two wavelengths.

3.3. Ground measurements obtained on May 29, 2008

On the cloudy day of May 29, 2008 the reference instrument (TriOS RAMSES-ACC-UV Hyperspectral UV/VIS

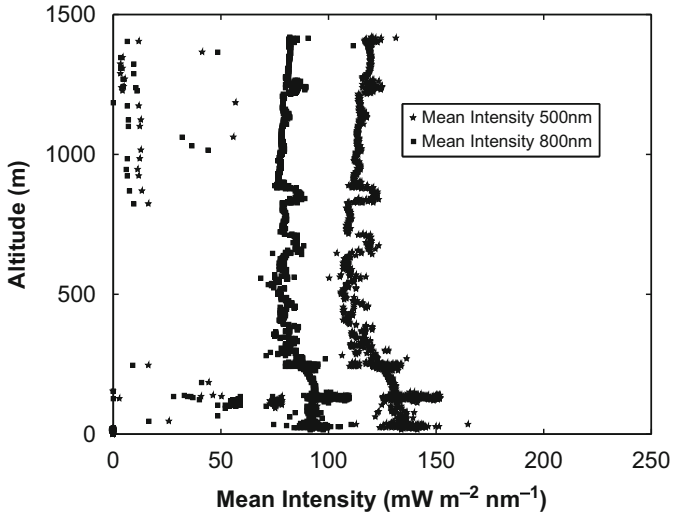

Fig. 5. Mean intensity measurements under clear-sky conditions on May 4, 2008. Stars represent measurements in the 500 nm channel and squares represent measurements in the 800 nm channel.

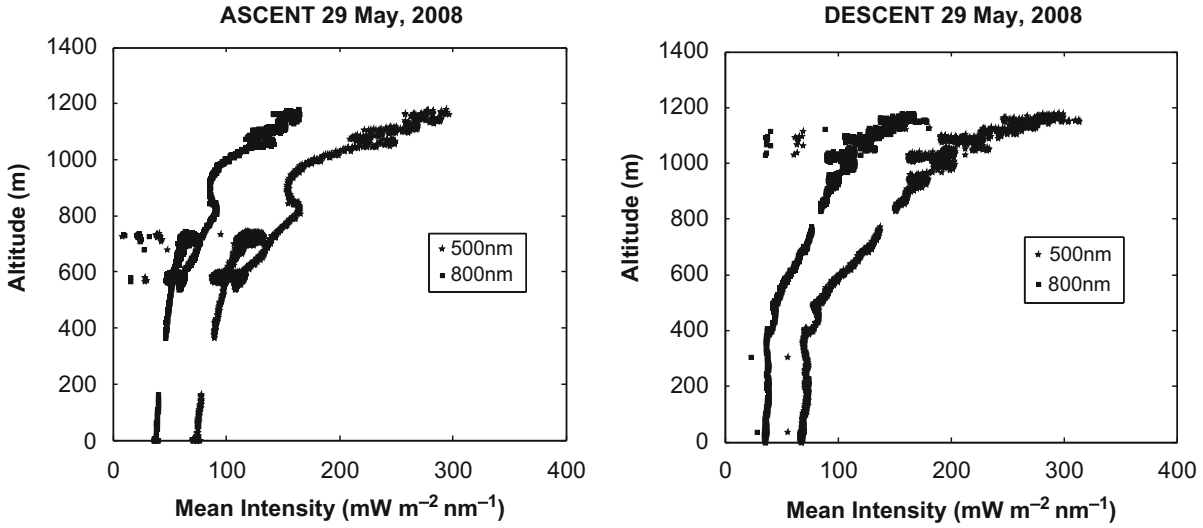

Fig. 6. Estimated mean intensity at 800 nm (left trace) and 500 nm (right trace) for cloudy sky conditions during ascent (left panel) and descent (right panel) on May 29, 2008.

Irradiance sensor) recorded the total downward irradiance [Fig. 7] from 10:57 UTC to 15:57 UTC at the ground every 5 min in the wavelength range between 319 and 915 μm, providing data that can be used to estimate the total optical depth of the cloud as a function of time. At any given time, the total cloud optical depth inferred from the ground radiometer and the 4π radiometer deployed on the TBS must be the same.

4. Model simulations

4.1. Radiative transfer model

To simulate the TBS and ground-based radiometric measurements we let the cloud be represented by vertically stratified layers of liquid droplets and ice particles, so that we could compute irradiances and mean intensities by using an azimuthally averaged version of the radiative transfer equation, which describes transfer of the diffuse monochromatic solar intensity I in a scattering and absorbing plane-parallel atmosphere:

$$u\frac{dI(\tau,u)}{d\tau} = I(\tau,u) - \frac{a(\tau)}{2}\int_{-1}^{1} du' p(\tau,u',u) I(\tau,u') - S^*(\tau,u). \qquad (1)$$

Here $d\tau(z) = -k(z)\,dz$, $\tau(z)$ is the non-dimensional optical depth, z is the altitude, $a(\tau(z)) = \sigma(z)/k(z)$ is the single-scattering albedo, $\sigma(z)$ is the scattering coefficient, $k(z)$ is extinction coefficient, $p(\tau,u',u)$ is the scattering phase function and $S^*(\tau,u)$ is the solar beam pseudo-source, which drives the diffuse radiation. Without $S^*(\tau,u)$ there would be no diffuse radiation. To incorporate clouds in a plane-parallel radiative transfer model we may use multiple stratified homogeneous layers. If we adopt a sufficiently large number of layers, this approach, which has been used in a number of studies (see e.g. Tsay et al. [12,13]), can account for significant vertical variations in

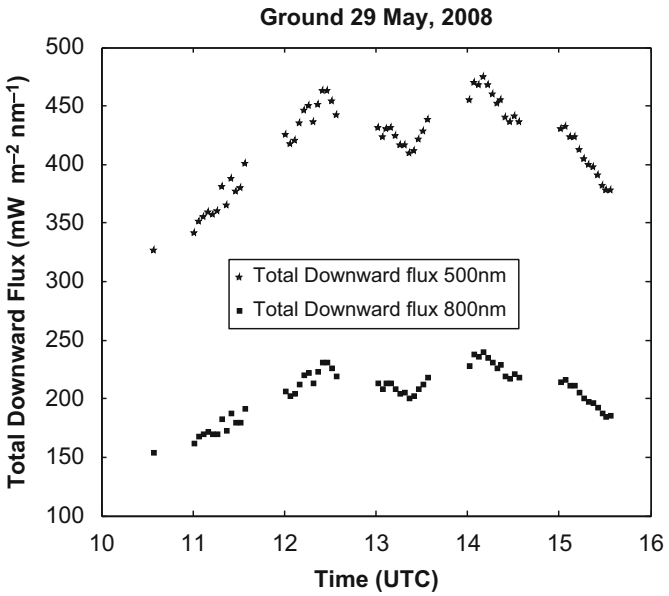

Fig. 7. Total downward irradiance at the ground at 500 nm (upper trace) and 800 nm (lower trace) versus time (i.e. changing solar zenith angle).

gaseous absorption and scattering as well as in the size distribution of water droplets and in the size and shape distributions of ice particles and their associated radiative effects. Based upon these considerations, we constructed a radiative transfer model that included radiative interactions with atmospheric gases (see Section 4.2.1) as well as parameterized treatments of scattering and absorption by cloud particles (see Section 4.2.2).

To solve the radiative transfer equation [Eq. (1)] we employed the radiative transfer code DISORT [7], which is well suited for our purpose. The input to the model included solar irradiance data obtained from NASA's Solar Radiation and Climate Experiment (SORCE) taken to be approximately 1900 mW m^{-2} nm^{-1} at 500 nm and 1100 mW m^{-2} nm^{-1} at 800 nm. Other input parameters included the cosine of the solar zenith angle calculated from http://www.srrb.noaa.gov/highlights/sunrise/azel.html (NOAA's solar calculator) and a Lambertian surface albedo, which was estimated from measurements taken under clear-sky conditions.

4.2. Inherent optical properties

4.2.1. Clear atmosphere

To estimate molecular absorption and scattering we used MODTRAN (MODerate resolution atmospheric TRANsmission), which is a computer program designed to simulate atmospheric propagation of electromagnetic radiation in the 100–50,000 cm^{-1} (0.2−100 μm) spectral range. We used 42 layers to represent the vertical variation of the atmospheric absorption with a height resolution of 100 m from the ground up to an altitude of 2000 m and with a coarser height resolution from there up to the top of the atmosphere at 70 km (see Fig. 8). The scattering optical depth $\tau_{scatter}$ and the total optical depth τ_{total} at 500 and 800 nm for molecular (Rayleigh) scattering and absorption in each of the 42 atmospheric layers were computed using MODTRAN.

To simulate the radiation field at the location of the 4π radiometer deployed on the TBS platform, the appropriate altitude to be used in the model was calculated from the pressure data collected by the meteorological package.

4.2.2. Cloud model

Fig. 8 shows the cloud layers embedded within the 42 layers of clear atmosphere. The CPI data helped in defining the structure of the cloud profile. Based upon CPI data from May 29, 2008 (Fig. 4) and the behavior of the measured irradiance on that day, we included two cloud layers, a lower layer stretching from 400 to 700 m and a higher layer stretching from 700 to 1200 m. Due to unknown conditions above the balloon's maximum height, we cannot guarantee the absence or presence of clouds above 1200 m. However, the sharp gradient seen in Fig. 6 indicates that we are very close to the top of the cloud. The CPI data for May 29, 2008 showed that there was ice mainly near the ground in the lower cloud layer and liquid water in the upper cloud layer. Since the optical depth usually decreases when liquid water transforms into the solid phase [14], the lower cloud layer is expected to be optically thinner than the higher cloud layer. The first moment of the scattering phase function, the so called asymmetry factor g, is often adopted to describe the radiative properties of clouds. The asymmetry factor and the single-scattering albedo of the cloud particles were parameterized on the basis of Mie theory [15]. We used the Henyey–Greenstein scattering phase function, which depends only on the asymmetry factor, to characterize the angular distribution of the scattered radiation. Since the asymmetry factor usually is smaller for ice than for water [1,15–17], we let the asymmetry factor for cloud particles in the lower ice-cloud layer be smaller (g=0.75) than in the higher liquid-water cloud layer (g=0.80).

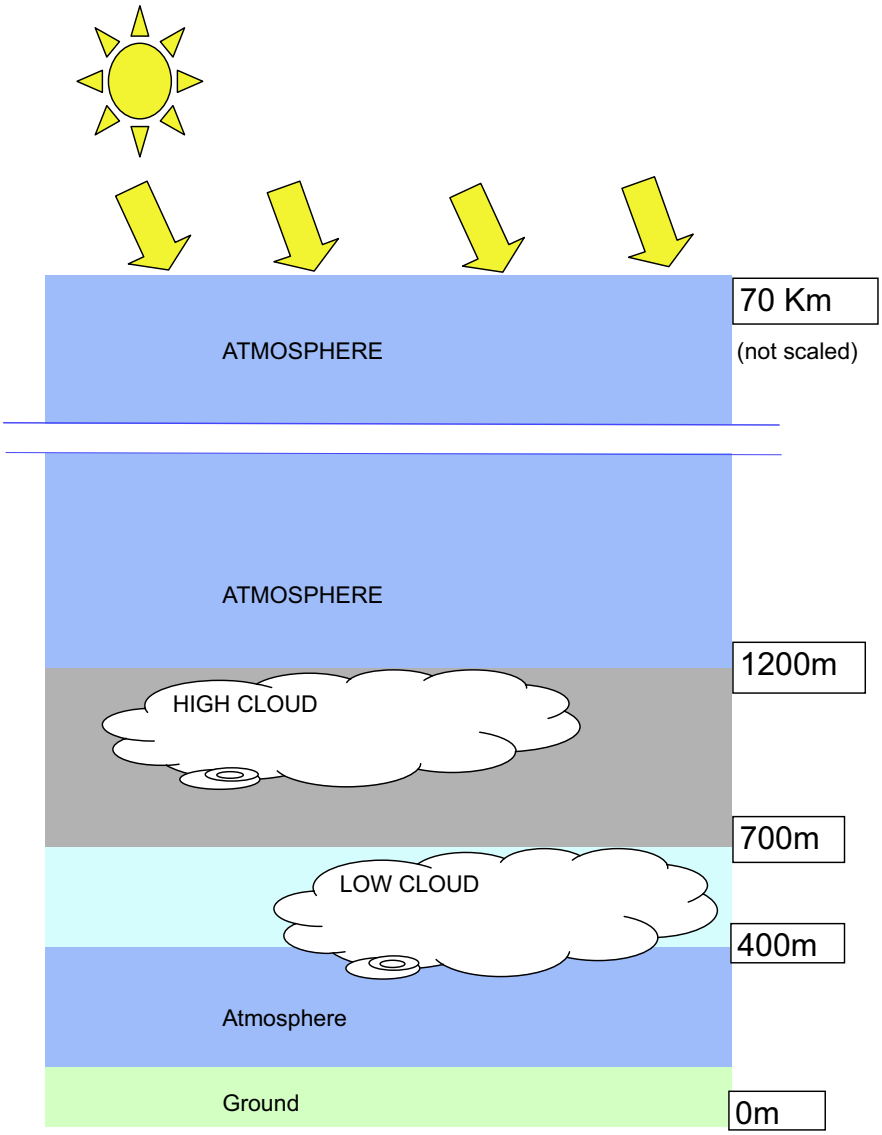

Fig. 8. Schematic illustration of the atmospheric model with two cloud layers embedded within the 42 atmospheric layers used to describe the clear-sky background.

The single-scattering albedo was assumed to be 0.999 both at 500 and 800 nm.

5. Results

The radiometric data obtained during the flight on May 29, 2008 under cloudy conditions were analyzed using the radiative transfer model described in Section 4. The optical properties of the cloud were represented by its optical depth, single-scattering albedo and asymmetry factor. As described in Section 4, we fixed the single-scattering albedo and the asymmetry factor for both cloud layers, but allowed the cloud optical depth to vary in the two atmospheric cloud layers. Fig. 9 shows a comparison of the total downward irradiance measured at the surface with the ground-based radiometer with that obtained from our simulations. The total cloud optical depth was varied in the model until agreement was obtained between measured and simulated irradiances at 500 and 800 nm, for which we have simultaneous measurements obtained with the 4π radiometer deployed on the TBS platform.

The total downward irradiance measured by the ground-based radiometer depends mainly on the total optical depth and is insensitive to its vertical distribution. Hence, it contains little information about the vertical cloud structure. But the mean intensity inferred from measurements by the 4π radiometer, deployed on the TBS platform inside the cloud, will be sensitive to the vertical cloud structure. By varying the optical depth of the lower and higher cloud layers until we get the best match between measured and simulated mean intensities, we obtain information about the vertical distribution of the optical depth within the cloud, while the total optical depth is constrained to be the same as that inferred from the ground-based radiometer data. Thus, simultaneous measurements of the total downward irradiance with the ground-based radiometer and the mean intensity with the

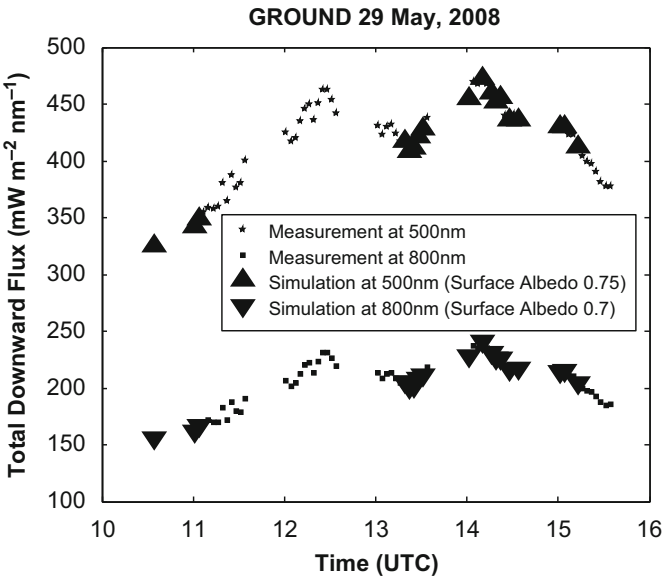

Fig. 9. Total downward irradiance as a function of time on the cloudy day of May 29, 2008 is shown at 500 nm (upper trace) and at 800 nm (lower trace). Simulated results are also shown.

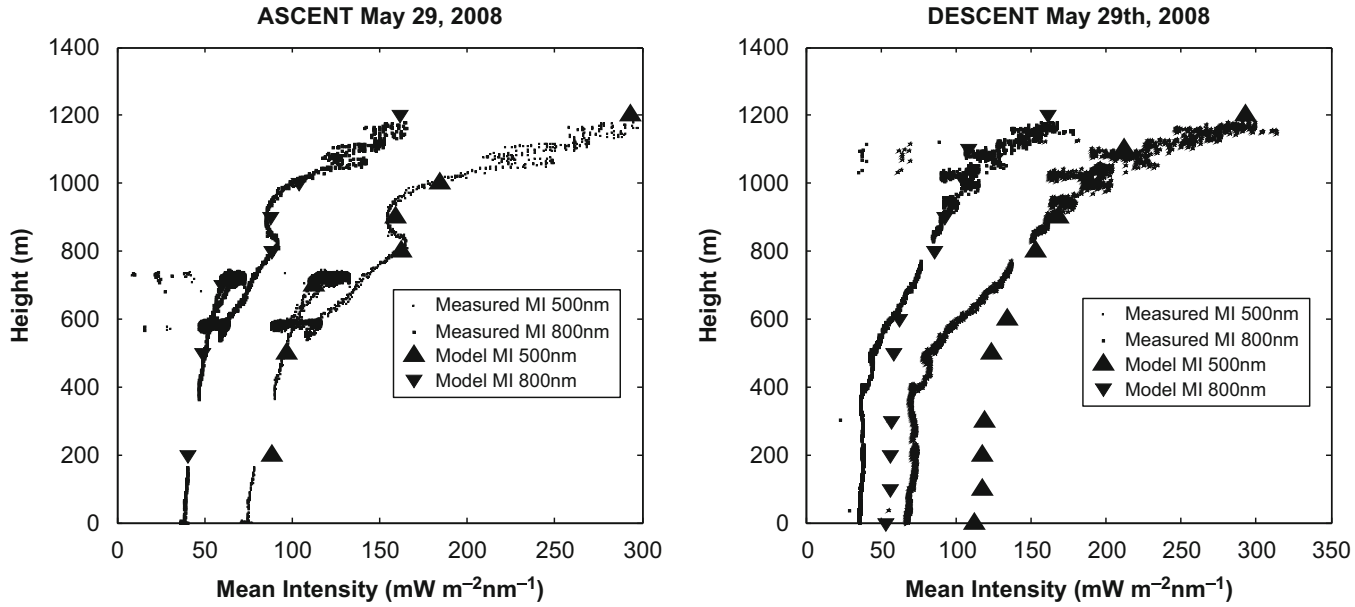

Fig. 10. Left: Variation of mean intensity (mW m^{-2} nm^{-1}) with height (in meters) at 500 and 800 nm during *ascent*. Right: Variation of mean intensity (mW m^{-2} nm^{-1}) with height (in meters) at 500 and 800 nm during *descent*. Values inferred from the measurements as well as simulated mean intensities giving the best matched to the measured data are shown.

in-cloud 4π radiometer allow us to estimate the fraction of the total optical depth that can be attributed to each of the lower and higher cloud layers.

Fig. 10 shows results of applying the procedure described above to estimate cloud structure during the ascent and descent of the TBS platform. In the left panel we display a comparison of simulated and measured mean intensities for the 500 nm channel of the 4π radiometer and the right panel displays comparison for the 800 nm channel. The comparisons are limited to simultaneous measurements obtained by the ground-based radiometer and the 4π radiometer deployed on the TBS platform. Fig. 11 shows the partitioning of the optical depth between the lower and higher cloud layer during the flight. These optical depths are obtained at a particular time or solar zenith angle by finding the best simultaneous match of the total optical depth estimated from the 4π measurements at that particular time (height) and from the total downward irradiance measured with upward-looking radiometer on the ground. Clearly, the upper liquid-water cloud layer was optically much thicker than the lower ice-cloud layer.

The simulated mean intensities were found to be in good agreement with those inferred from the measured 4π radiometer data for the flight conducted during cloudy conditions on May 29, 2008. As a result of this analysis we

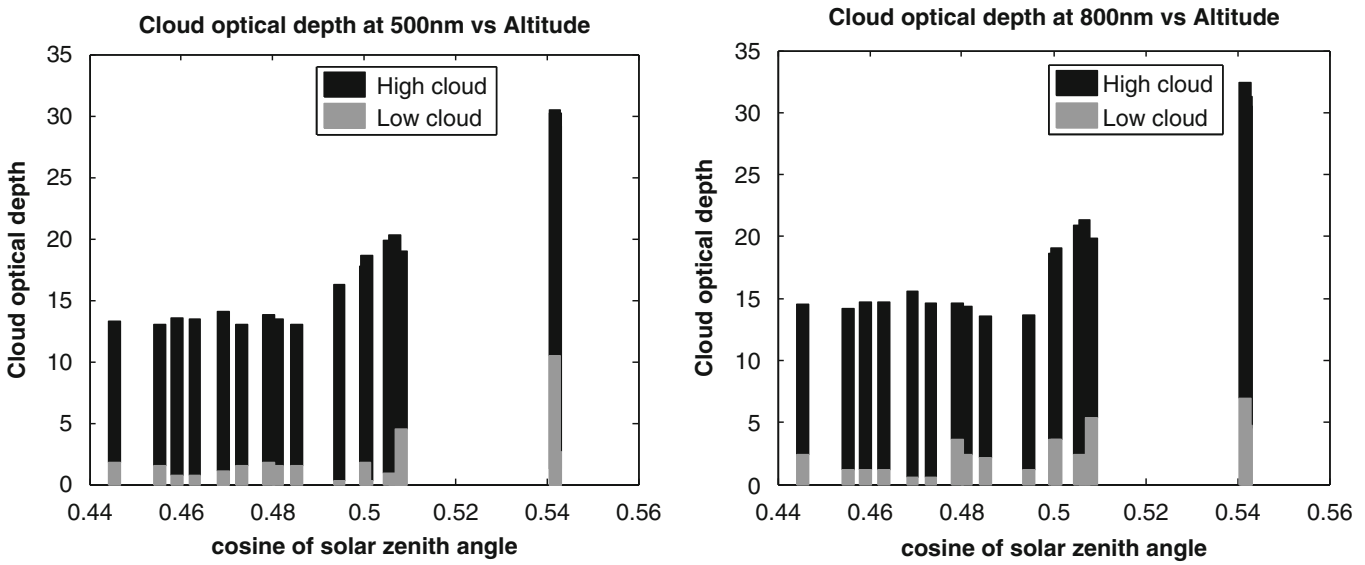

Fig. 11. Left: Varying optical depth at 500 nm for the two cloud layers. Right: Varying optical depth at 800 nm for the two cloud layers. The lower bar (gray) shows the optical depth of the lower cloud layer, while the upper stacked bar (black) shows the optical depth of the upper cloud layer during the flight.

found that there is better agreement between modeled and measured mean intensities within thick clouds. This circumstance can be attributed to the predominance of diffuse radiation in optically thick clouds. We also found that the maximum total cloud optical depth inferred from the data collected on May 29 was approximately 31 at 500 nm and approximately 32 at 800 nm. Furthermore, we see from Fig. 10 that there is close agreement between modeled and measured mean intensities during the ascent. On the other hand, during balloon descent there is considerable disagreement between simulated and measured mean intensities near the ground. A possible reason for this discrepancy could be that a small amount of riming formed as the balloon descended on May 29, 2008 (see Fig. 2). Such riming would be expected to reduce the sensitivity of the 4π radiometer and would help explain the difference between simulated and measured mean intensities towards the end of the balloon flight during descent.

6. Summary and outlook

A novel system has been developed for *in situ* measurements of cloud microphysical and radiative properties. This system is capable of measuring true vertical profiles and time series of microphysical and radiometric properties. Such *in situ* measurements are not feasible using aircraft or ground-based remote sensing instruments only. The powered tether approach allows for long time series and uninterrupted operation. This feature is especially valuable in cold climates where battery lifetime is limited. The radiometric data collected in May 2008 at Ny-Ålesund via two instruments, namely the NILU-CUBE 4π radiometer on the balloon flight and the RAMSES radiometer on the ground, were analysed to retrieve optical properties of a mixed-phase cloud. For this purpose a radiation model was constructed that included scattering and absorption by both molecules and cloud particles.

Our analysis of the radiometer data for the flight on May 29, 2008 can be summarized as follows:

- there was better agreement between simulated and measured mean intensities within thick clouds, which we attribute to the enhanced presence of diffuse radiation in optically thick clouds;
- the maximum total cloud optical depth observed on May 29, 2008 was approximately 31 at 500 nm and approximately 32 at 800 nm;
- there was close agreement between simulated and measured mean intensities during the ascent;
- during balloon descent there was considerable disagreement between simulated and measured mean intensities near the ground. A small amount of riming formed as the balloon descended could be the reason for reduced sensitivity of the 4π radiometer during the descent.

The TBS is a platform that can be used to deploy a variety of instrument packages into the atmospheric boundary layer including cloud condensation nuclei (CCN) and ice forming nuclei (IFN) counters as well as cameras for monitoring the surface conditions, filters for collecting and analyzing ice nuclei, a particle imaging probe that extends to cm-size particles and a new miniaturized (<2 kg) *in situ* cloud lidar currently under development.

The CPI used in the current TBS weighs 7 kg. A miniature CPI, designed to fly on a small, unmanned aerial system, is now under development and weighs less than 2 kg. Adoption of this new CPI technology into the TBS, would increase the payload potential by 5 kg and

thus enable one to add new instruments, such as those discussed above.

The current 4π radiometer has only two channels. It would be valuable to build a next-generation radiometer that would include additional near-infrared channels.

The present winch, built for the 1998 SHEBA project, was dimensioned for a tether designed to carry high currents that would heat the tether for deicing purposes. The high-current approach necessitated a large drum that would provide large surface area exposure for adequate cooling of the tether. It was found that the high current was unnecessary for deicing and a lower-current approach was subsequently adopted. Since the high current and large drum are no longer needed, a smaller drum could be fabricated that would considerably reduce the size and weight of the TBS and allow it to be transported on commercial airliners with limited cargo door access dimensions.

Finally, it would be useful to develop reliable data processing tools that could be used to turn the data collected by the TBS instruments into meaningful geophysical parameters. For example, flow modeling and calibration techniques need to be developed to better quantify CPI collection efficiency of water and ice particles, which is a complex solution of particle type and size, fall velocity, ambient wind speed and sample tube angle of attack. Quantified water drop and ice particle size distributions would then be used to compute total water drop and ice particle concentrations, liquid water content (LWC), ice water content (IWC), effective radii and extinction coefficients and combined values of these parameters. The asymmetry parameter, can be derived from Mie scattering theory for the liquid water drop portion of the cloud and from lookup tables that relate CPI particle shape to the scattering phase function for the ice portion of the cloud [18,19]. Also, data collected with the 4π radiometer, as discussed in this paper, in conjunction with the CPI data can be used to infer the total optical depth and its partitioning between liquid water and ice. These optical properties (effective particle size, ice water path, extinction coefficient, optical depth and asymmetry parameter) which can be derived from future TBS measurements, are the inputs required by climate models.

To put future TBS measurements into perspective, we close by noting that a proper treatment of clouds in the Arctic is a prerequisite for reliable estimates of climate forcing, the onset of snowmelt, the rate of snow/ice ablation, the length of the melt season [20,21] and ultimately the fate of sea ice and ice sheets in a changing climate.

Acknowledgements

This work was supported by the National Science Foundation (NSF) Physical Meteorology Program Grant no. ATM-0752893 to Stevens Institute of Technology as well as through NSF Grant DGE-0742462 supporting GK-12 fellowships. The work was also supported by the Norwegian Research Council through its International Polar Year programme and the project IPY-THORPEX (Grant number 175992/S30, www.ipy-thorpex.no). The support of the National Science Foundation and the Norwegian Research Council is gratefully acknowledged.

References

[1] Kahnert M, Sandvik AD, Biryulina M, Stamnes J, Stamnes K. Impact of ice particle shape on short-wave radiative forcing: a case study for an arctic ice cloud. J Quant Spectrosc Radiat Transfer 2008;109:1196–218.
[2] Ramanathan V, Barkstrom BR, Harrison EF. Climate and the earth's radiation budget. Int Agrophys 1989;5(3–4):171–81.
[3] Lawson RP, Baker BA, Schmitt CG, Jensen TL. An overview of microphysical properties of Arctic clouds observed in May and July 1998 during FIRE ACE. J Geophys Res 2001;106:14989–5014.
[4] Verlinde J, Harrington JY, Mcfarquha GM, Yannuzzi VT, Avramov A, Greenberg S, et al. The mixed phase arctic cloud experiment. Am Meteorol Soc 2007;88:205–21.
[5] Storvold R, Stamnes K. Development and deployment of a powered tethered balloon system at the SHEBA ice station for measurements of cloud micro-physical and radiative properties. In: Proceedings of the ninth ARM science team meeting, March 22–26, San Antonio, Texas, 1999.
[6] Holland MM, Bitz CM. Polar amplification of climate change in coupled models. Clim Dyn 2003;21:221–32.
[7] Stamnes K, Tsay SC, Wiscombe WJ, Jayaweera K. Numerically stable algorithm for discrete-ordinate-method radiative transfer in multiple scattering and emitting layered media. Appl Opt 1988;27:2502–9.
[8] Koskulics J, Sikand M, Stamnes K, Hamre B, Stamnes J, Lawson RP. Flux magnitude and mean intensity measured with an airborne NILU cube radiometer: Selected cases of boundary layer arctic stratus clouds. J Quant Spectrosc Radiat Transfer, 2010, in preparation.
[9] Lawson RP, Stamnes K, Stamnes JJ, Zmarzly P, Koskuliks J, Roden C, et al. Deployment of a tethered balloon system for cloud microphysics and radiative measurements at Ny-lesund and south pole. J Atmos Ocean Tech submitted 2010.
[10] Madronich S. Photodissociation in the atmosphere 1. Actinic flux and the effects of ground reflections and clouds. J Geophys Res 1987;92:9740–52.
[11] de Arellano JVG, Duynkerke PG, Weele MV. Tethered-balloon measurements of actinic flux in a cloud-capped marine boundary layer. J Geophys Res 1994;99:3699–705.
[12] Tsay SC, Stamnes K, Jayaweera K. Radiative energy budget in the cloudy and hazy Arctic. J Atmos Sci 1989;46:1002–18.
[13] Tsay SC, Stamnes K, Jayaweera K. Radiative transfer in stratified atmospheres: description and validation of a unified model. J Quant Spectrosc Radiat Transfer 1990;43:133–48.
[14] Curry JA, Ebert EE. Annual cycle of radiative fluxes over the Arctic Ocean: sensitivity to cloud optical properties. J Clim 1992;5:1267–80.
[15] Hu Y, Stamnes K. An accurate parameterization of the radiative properties of water clouds suitable for use in climate models. J Clim 1993;6:728–42.
[16] Sun Z, Shine K. Studies of the radiative properties of ice and mixed-phase clouds. Quart J Roy Meteor Soc 1994;120:111–37.
[17] Fu Q. An accurate parameterization of the solar radiative properties of cirrus clouds for the climate models. J Clim 1996;9:2058–82.
[18] Lawson RP, Heymsfield AJ, Aulenbach SM, Jensen TL. Shapes, sizes and light scattering properties of ice crystals in cirrus and a persistent contrail during SUCCESS. Geophys Res Lett 1988;25:1331–4.
[19] Shcherbakov V, Gayet JF, Baker B, Lawson RP. Light scattering by single natural ice crystals. J Atmos Sci 2006;63:1513–25.
[20] Zhang T, Stamnes K, Bowling SA. Impact of clouds on surface radiative fluxes and snow melt in the Arctic and Subarctic. J Clim 1996;9:2110–23.
[21] Zhang T, Bowling SA, Stamnes K. Impact of the atmosphere on surface radiative fluxes and snow melt in the Arctic and Subarctic. J Geophys Res 1997;102:4287–302.